



Article

Convergence Analysis of Iterative Learning Control for Initialized Fractional Order Systems

Xiaofeng Xu , Jiangan Lu * and Jinshui Chen

State Key Laboratory of Industrial Control Technology, College of Control Science and Engineering, Zhejiang University, Hangzhou 310027, China; xxf_cse@zju.edu.cn (X.X.); jschen@zju.edu.cn (J.C.)

* Correspondence: lujg@zju.edu.cn

Abstract: Iterative learning control is widely applied to address the tracking problem of dynamic systems. Although this strategy can be applied to fractional order systems, most existing studies neglected the impact of the system initialization on operation repeatability, which is a critical issue since memory effect is inherent for fractional operators. In response to the above deficiencies, this paper derives robust convergence conditions for iterative learning control under non-repetitive initialization functions, where the bound of the final tracking error depends on the shift degree of the initialization function. Model nonlinearity, initial error, and channel noises are also discussed in the derivation. On this basis, a novel initialization learning strategy is proposed to obtain perfect tracking performance and desired initialization trajectory simultaneously, providing a new approach for fractional order system design. Finally, two numerical examples are presented to illustrate the theoretical results and their potential applications.

Keywords: fractional calculus; iterative learning control; convergence analysis; initialization learning



Citation: Xu, X.; Lu, J.; Chen, J. Convergence Analysis of Iterative Learning Control for Initialized Fractional Order Systems. *Fractal Fract.* **2024**, *8*, 168. <https://doi.org/10.3390/fractalfract8030168>

Academic Editors: António Lopes, Ernesto Zambrano-Serrano, Miguel A. Platas-Garza and Cornelio Posadas-Castillo

Received: 20 January 2024
Revised: 8 March 2024
Accepted: 10 March 2024
Published: 14 March 2024



Copyright: © 2024 by the authors. Licensee MDPI, Basel, Switzerland. This article is an open access article distributed under the terms and conditions of the Creative Commons Attribution (CC BY) license (<https://creativecommons.org/licenses/by/4.0/>).

1. Introduction

The concept of fractional order iterative learning control (FOILC) [1] has two meanings, where the fractional order can be derived from both the plant control system and the iterative learning law. This topic has significant research value, because fractional order systems have been verified in some important disciplines, such as secondary batteries [2] and materials science [3]; and for iterative learning control (ILC), the fractional order operator has also been proven to help improve the convergence characteristics of the system [4,5].

The initial state issue is a hot spot in ILC research [6], and its criticality can be explained from two aspects. On the one hand, the initial error significantly affects the final tracking performance; on the other hand, the possible non-repetition of the initial value also breaks the strict repeatability requirements of ILC for the plant system [7]. To the best of our knowledge, there are two main mathematical methods for dealing with the unavoidable initial errors. The first is to derive robust convergence conditions by adjusting the control structure or system assumptions [8–10]; and the second is to design adaptive correction algorithms to eliminate the impact of initial shift, such as initial state learning [11] and rectifying actions [12,13].

In the field of FOILC, the initial state issue has been investigated under different complex system dynamics and assumptions, such as time-delay [14], multi-agent systems [15,16], nonuniform pass lengths [17], and internal models [18]. Although most of the above learning- [19] or rectification-based [20] methods can be extended to fractional order systems, a hidden but significant issue has been neglected. Due to the historical correlation of the fractional operator, the initial values of fractional order systems are theoretically infinite dimensional [21], and a history function defined on the initialization domain is required to fully initialize the fractional order system [22]. However, in most

cases, only finite dimensional initial states are considered in ILC design. If such ILC strategies are directly applied to fractional order systems, it may inevitably lead to the loss of initialization information.

The significance of considering complete initialization for fractional order systems has been revealed in both mathematics and engineering applications. For example, the initialization approach has been proven to be related to the response [23] and solution properties [24] of the system, while in material mechanics [25] and fractional order circuits [26], the significance of preprocessing has also been recognized. However, in the field of ILC, there have been no notable achievements for initialized fractional order systems. Since the initialization function is more complex than finite dimensional initial state, the analysis of ILC convergence is challenging, especially when the initialization process is perturbed or not repeated. The degree to which the initialization shift breaks the tracking performance has not been theoretically clarified. In this regard, refs. [27,28] proposed a system preconditioning strategy based on the short memory principle to improve the system performance and then derived the ILC convergence condition. However, this ILC scheme cannot achieve perfect tracking performance, and the preconditioning operation requires additional time cost.

Inspired by the existing deficiencies, this paper investigates the ILC problem of initialized fractional order systems, fully explores the impact of initialization factors on tracking performance of the iterative system, and designs control strategies to improve the convergence properties. To achieve these targets, the following methodologies are adopted. First, under the framework of initialized fractional order nonlinear system, the ILC problem is specified and the causality between system initialization and initial states is established, the operating interval is extended to the entire initialization stage. Subsequently, the convergence properties of the tracking errors are derived based on norm and contraction mapping methods. Under a close-loop D^α -type ILC updating law, the boundedness conditions of the tracking errors are obtained, and the algorithmic factors affecting the error level are theoretically analyzed. Finally, under the condition that the initialization trajectory can be addressed, a novel initialization learning algorithm is proposed to eliminate the initialization shift and thus achieve perfect tracking performance.

The paper includes the following innovative contributions.

- (a) This study reveals how and to what extent system initialization weakens the ideal convergence of ILC, and a novel ILC robust convergence condition for initialized fractional order systems is strictly derived.
- (b) Combining the ILC tracking problem with the optimization of system initialization, a novel initialization learning strategy is proposed and applied to ensure the perfect tracking of ILC.
- (c) The results have broad applicability and better physical interpretability compared with existing literature, as complex system dynamics such as nonlinearity and channel noises are involved, and the connection between initialization and initial states is theoretically clarified.

The rest of this paper is organized as follows. Necessary preliminaries are presented in Section 2. The ILC problem for initialized fractional order system is stated and discussed in Section 3. Mathematical results are derived in Section 4. Numerical examples and conclusions are elaborated in Sections 5 and 6.

2. Preliminaries

In this section, some necessary definitions and lemmas are presented. The Caputo-type fractional operator is adopted in this paper because it has integer order initial values, and is physically interpretable in real-world models [29].

Definition 1 (Fractional integral, [30]). The fractional integral of an integrable function $f(t): [t_0, +\infty) \rightarrow \mathbb{R}^n$ with order $\alpha \in (0, 1)$ is defined as

$${}_t D_t^{-\alpha} f(t) = \int_{t_0}^t \frac{(t-s)^{\alpha-1}}{\Gamma(\alpha)} f(s) ds \quad (1)$$

if (1) converges pointwisely on $(t_0, +\infty)$, where $\Gamma(\cdot)$ denotes the Gamma function.

Definition 2 (Fractional derivative). The Caputo-type fractional derivative of a piecewise smooth function $f(t): [t_0, +\infty) \rightarrow \mathbb{R}^n$ with order $\alpha \in (0, 1)$ is defined as

$${}_t^C D_t^\alpha f(t) = {}_t D_t^{-(1-\alpha)} \left[\frac{d}{dt} f(t) \right] = \int_{t_0}^t \frac{(t-s)^{-\alpha}}{\Gamma(1-\alpha)} \frac{d}{ds} f(s) ds \quad (2)$$

if (2) converges pointwisely on $(t_0, +\infty)$.

It can be seen from Definitions 1 and 2 that the fractional operators has nonlocal property, i.e., the derivative value of f at time t is related to the function history over the entire interval $[t_0, t]$. In most FOILC studies, the fractional derivative is defined on the operating interval of the iterative system, usually a fixed $[0, T]$. However, this approach will lead to the loss of physical information if significant history states, such as system preheating and reposition, are contained before $t = 0$. For a state trajectory $f(t)$ defined on $[0, T]$, suppose that the history states are described by the history function $\phi(t)$, where $t \in [t_0, 0)$. Then, according to (2), the Caputo derivative of f containing all history information can be written as

$${}_0^C D_t^\alpha f(t) = {}_t^C D_t^\alpha f(t) = \int_{t_0}^0 \frac{(t-s)^{-\alpha}}{\Gamma(1-\alpha)} \frac{d}{ds} \phi(s) ds + \int_0^t \frac{(t-s)^{-\alpha}}{\Gamma(1-\alpha)} \frac{d}{ds} f(s) ds, \quad (3)$$

where ${}_0^C D_t^\alpha$ denotes the Caputo-type initialized fractional operator, $\alpha \in (0, 1)$, $t \in [0, T]$. The second term on the right side of (3) is actually ${}_0^C D_t^\alpha f(t)$, and the first term is called the initialization function [31]:

$$\Psi(\phi, \alpha, t_0, 0, t) = \int_{t_0}^0 \frac{(t-s)^{-\alpha}}{\Gamma(1-\alpha)} \frac{d}{ds} \phi(s) ds. \quad (4)$$

Thus, (3) can be rewritten as follows:

$${}_0^C D_t^\alpha f(t) = \Psi(\phi, \alpha, t_0, 0, t) + {}_0^C D_t^\alpha f(t), \quad (5)$$

It can be seen that the initialization function Ψ actually extends the domain of the fractional operator from $[0, T]$ to $[t_0, T]$, and formally maintains the consistency between the operator's definition interval and the operating interval. Dynamic systems defined by the initialized fractional operator are called initialized fractional order systems.

The introduction of Ψ brings new complex system dynamics and challenges to control design, which will be discussed in detail in Section 3. Here, a few critical preliminaries are given. First, to evaluate the system performance over a certain interval, the definition of λ -norm is introduced as follows.

Definition 3. For a function $f: [0, T] \rightarrow \mathbb{R}^n$, the λ -norm is defined as:

$$\|f\|_\lambda = \sup_{t \in [0, T]} \left\{ e^{-\lambda t} \|f(t)\|_\infty \right\}, \quad (6)$$

where $\lambda > 0$ is a constant, $\|\cdot\|_\infty$ denotes the infinite norm.

In addition, Lemma 1 provides the relationship between functions and their fractional integrals in the sense of ∞ -norm and λ -norm.

Lemma 1. Suppose that $Y(t)$ is an arbitrary fractional integrable function defined on $[0, T]$, given a constant $\lambda > 0$, then

$$\| {}_0D_t^{-\alpha} Y(t) \|_{\infty} \leq \frac{e^{\lambda t}}{\lambda^{\alpha}} \cdot \| Y \|_{\lambda}, \quad (7)$$

where $\alpha \in (0, 1)$. Furthermore, for the λ -norm of Y , the following inequality holds:

$$\| {}_0D_t^{-\alpha} Y(t) \|_{\lambda} \leq \frac{1}{\lambda^{\alpha}} \cdot \| Y \|_{\lambda}. \quad (8)$$

Proof. It follows from (1) that

$$\| {}_0D_t^{-\alpha} Y(t) \|_{\infty} \leq \int_0^t \frac{(t-s)^{\alpha-1}}{\Gamma(\alpha)} \| Y(s) \|_{\infty} ds \leq \int_0^t \frac{e^{\lambda s} (t-s)^{\alpha-1}}{\Gamma(\alpha)} ds \cdot \| Y \|_{\lambda}, \quad (9)$$

applying Inequality (10) (see proof of Theorem 3.3, [32]) to (9), it is easy to see that (7) holds:

$$\int_0^t (t-s)^{\alpha-1} e^{\lambda s} ds \leq \frac{\Gamma(\alpha) e^{\lambda t}}{\lambda^{\alpha}}. \quad (10)$$

Then, applying the λ -norm and (7) to ${}_0D_t^{-\alpha} Y(t)$ yields

$$\begin{aligned} \| {}_0D_t^{-\alpha} Y(t) \|_{\lambda} &= \sup_{t \in [0, T]} \{ e^{-\lambda t} \cdot \| {}_0D_t^{-\alpha} Y(t) \|_{\infty} \} \\ &\leq \sup_{t \in [0, T]} \{ e^{-\lambda t} \cdot \frac{e^{\lambda t}}{\lambda^{\alpha}} \| Y \|_{\lambda} \} = \frac{1}{\lambda^{\alpha}} \cdot \| Y \|_{\lambda}, \end{aligned} \quad (11)$$

which means that (8) holds as well. \square

Finally, the following Lemmas 2 and 3 are cited to evaluate the state of iterative systems, which are also necessary in the ILC convergence analysis.

Lemma 2 (Generalized Grönwall–Bellman inequality, [33]). Suppose that $\alpha > 0$, $w(t)$ is nonnegative and locally integrable on $[0, T]$ ($0 < T < \infty$), and $g(t)$ is nonnegative, nondecreasing, continuous and no greater than a constant M on $[0, T]$. If $u(t)$ is nonnegative, locally integrable and satisfies

$$u(t) \leq w(t) + g(t) \cdot \int_0^t (t-s)^{\alpha-1} u(s) ds \quad (12)$$

on $[0, T]$, then

$$u(t) \leq w(t) + \int_0^t \sum_{n=1}^{\infty} \frac{(g(t)\Gamma(\alpha))^n}{\Gamma(n\alpha)} (t-s)^{n\alpha-1} w(s) ds. \quad (13)$$

In addition, if $w(t)$ is further nondecreasing on $[0, T]$, then

$$u(t) \leq w(t) \cdot E_{\alpha}(g(t)\Gamma(\alpha)t^{\alpha}), \quad (14)$$

where $E_{\alpha}(\beta) = \sum_{k=0}^{\infty} \frac{\beta^k}{\Gamma(k\alpha+1)}$ denotes the single-parameter Mittag–Leffler function.

Lemma 3 (see Lemma 1 and Lemma 2, [7]). For the following iterative system,

$$\theta_{l+1} = \Theta_l \theta_l + \sigma_l, \quad (15)$$

where $l \in \mathbb{N}$, $\theta \in \mathbb{R}^n$ is the state, $\sigma \in \mathbb{R}^r$ is the external input. Assume that the initial state θ_0 is bounded, the mapping matrix Θ satisfies $\|\Theta_l\| \leq \chi < 1$, where χ is a constant. If the input σ is bounded such that $\|\sigma_l\| \leq \beta_\sigma$ for some $\beta_\sigma > 0$, then

- a. θ_l is bounded such that $\sup_{l \in \mathbb{N}} \|\theta_l\| \leq \beta_\theta$ for some bounded $\beta_\theta > 0$.
- b. $\lim_{l \rightarrow \infty} \theta_l = 0$ if $\lim_{l \rightarrow \infty} \sigma_l = 0$.

3. Problem Statement

Many traditional ILC and FOILC problems have the following form: for a system operating repeatedly on a fixed $[0, T]$, designing an iterative learning law, so that the input–output pair (u_k, y_k) ($k \in \mathbb{N}$) converges to the reference pair (u_d, y_d) through the iterations. To achieve this target, the existence and uniqueness assumption of the reference system, i.e., (u_d, y_d) , is typically required. In this case, the convergence of u_k and y_k is equivalent. However, the situation is more complex for initialized fractional order systems. For a general input–output dynamic system,

$$\begin{aligned} {}_0^C D_t^\alpha y(t) &= f(y_k, u_k, t) \\ \text{or } {}_0^C D_t^\alpha y(t) &= -\Psi(\phi_k, \alpha, t_0, 0, t) + f(y_k, u_k, t), \end{aligned} \tag{16}$$

the history function ϕ_k changes the system dynamics and breaks the input–output uniformity. This is an assignable factor for ILC issues. On the one hand, the iterative algorithm may be invalid if ϕ_k varies for different k , an inappropriate initialization path may also leads to an initial error and thus damages the ILC performance. On the other hand, ϕ_k needs to be optimized in some practical cases. For example, in battery tests (see Example 1, Section 5), resting is a notable initialization method; while in viscoelasticity, it is required to design periodic excitation with specific amplitude and frequency [25,34]. The tracking of ϕ_d is usually necessary in the above scenarios.

In this paper, the following initialized fractional-order nonlinear system is considered:

$$\begin{cases} {}_0 D_t^\alpha x_k(t) = f(x_k(t), t) + Bu_k(t), \\ y_k(t) = Cx_k(t) + D \int_0^t g(s, u_k(s)) ds, \end{cases} \tag{17}$$

where $\alpha \in (0, 1)$, $x \in \mathbb{R}^n$ is the state, $u \in \mathbb{R}^r$ is the input, $y \in \mathbb{R}^m$ is the output, $g : [0, T] \times \mathbb{R}^n \rightarrow \mathbb{R}^p$, f, B and C have appropriate dimensions. f and g is Lipschitz continuous on $[0, T]$ with respect to t , i.e., $\|f(x_1(t), t) - f(x_2(t), t)\|_\infty \leq L_1 \|x_1(t) - x_2(t)\|_\infty$ for $t \in [0, T]$, $\|g(t, u_1(t)) - g(t, u_2(t))\|_\infty \leq L_2 \|u_1(t) - u_2(t)\|_\infty$. The system is initialized by a history function $\phi_k(t) : [t_0, 0) \rightarrow \mathbb{R}^n$ and the initialization function $\Psi(\phi_k, \alpha, t_0, 0, t)$ is abbreviated as $\Psi_k(t)$. The limit value of $\phi_k(t)$ at $t = 0_-$ is assumed to be the initial state $x_k(0)$; this is because physically the initial value should be considered as the result of the initialization operation.

Suppose that (ϕ_d, u_d, y_d) is the solution of the reference system

$$\begin{cases} {}_0 D_t^\alpha x_d(t) = f(x_d(t), t) + Bu_d(t), \\ y_d(t) = Cx_d(t) + D \int_0^t g(s, u_d(s)) ds \end{cases} \tag{18}$$

and meets the condition of existence and uniqueness. Then, the ILC tracking problem is to design an iterative algorithm to find a (ϕ_k, u_k, y_k) sequence, such that (u_k, y_k) converges to (u_d, y_d) as k increases. It can be seen from the above discussion that the history function is a generalization of the initial states. Therefore, similar to the well-known initial value issue, the initialization problems are proposed as follows and analyzed in Section 4.

- a. If ϕ_k is iteration-varying and thus leads to a non-repetitive initial shift, can ILC convergence be guaranteed? What conditions are required?
- b. Without considering the disturbances, if the initial history function $\phi_0 \neq \phi_d$, how to ensure that (u_k, y_k) simultaneously converges to the ideal (u_d, y_d) ?

4. Main Results

4.1. Bounded Tracking Error for Bounded Iteration-Varying Initialization

This section aims to derive the convergence conditions of bounded tracking errors from bounded initialization shift. More generally, the additive disturbances of the state equation and output channel are also considered. The system expression is presented as follows:

$$\begin{cases} {}_0D_t^\alpha x_k(t) = -\Psi_k(t) + f(x_k(t), t) + Bu_k(t) + \omega_k(t), \\ y_k(t) = Cx_k(t) + D \int_0^t g(s, u_k(s)) ds + v_k(t), \\ e_k(t) = y_d(t) - y_k(t), \end{cases} \quad (19)$$

where $\omega_k \in \mathbb{R}^n$ and $v_k \in \mathbb{R}^m$ denote the iteration-varying shift of the state and output equations. Under an arbitrary bounded initial $u_0(t)$ ($t \in [0, T]$), the following close-loop D^α -type updating law is adopted for iterations:

$$u_{k+1}(t) = u_k(t) + \Lambda \cdot {}_0D_t^\alpha e_{k+1}(t). \quad (20)$$

Here, the close-loop error $e_{k+1}(t)$ is introduced to enhance the robustness of the system, while the D^α -operator is adopted to achieve better convergence performance [35]. In addition, the following assumptions are required.

- (A) For all $k \in \mathbb{N}$, $\|\phi_d(t) - \phi_k(t)\|_\infty$ is bounded on $[t_0, 0)$; this assumption also indicates $\|\delta x_k(0)\|_\infty = \|x_d(0) - x_k(0)\|_\infty$ is bounded since $\lim_{t \rightarrow 0^-} \phi(t) = x(0)$.
- (B) The tracking error of $\phi_k(t)$ has a bounded growth speed, i.e., $\|\dot{\phi}_d(t) - \dot{\phi}_k(t)\|_\infty \leq M$, where M is a constant, $t \in [t_0, 0)$.
- (C) $\omega_k(t)$, $v_k(t)$, and $\dot{v}_k(t)$ are bounded on $[0, T]$.

The boundedness condition for tracking error of (u_k, y_k) is derived in four steps below. First, the iterative relationship of the tracking errors is established based on the ILC updating law. Then, the norm-based method is adopted to evaluate the error size, and the generalized Grönwall inequality is applied to address the variable coupling. Finally, the convergence conditions for the iterative system can be found.

Step 1. First, consider the convergence performance of u_k . The tracking error between u_k and u_d is denoted as δu_k , then it follows from (20) that

$$\begin{aligned} \delta u_{k+1}(t) &= u_d(t) - u_{k+1}(t) \\ &= \delta u_k(t) - \Lambda \cdot {}_0D_t^\alpha e_{k+1}(t) \\ &= \delta u_k(t) - \Lambda \cdot {}_0D_t^\alpha [y_d(t) - y_{k+1}(t)], \end{aligned} \quad (21)$$

replacing y_d and y_{k+1} with the output equations of (18) and (19) yields

$$\delta u_{k+1}(t) = \delta u_k(t) - \Lambda \cdot {}_0D_t^\alpha \{C\delta x_{k+1}(t) + D \int_0^t [g(s, u_d) - g(s, u_{k+1})] ds - v_{k+1}(t)\}, \quad (22)$$

where $\delta x_{k+1}(t) = x_d(t) - x_{k+1}(t)$. ${}_0D_t^\alpha \delta x_{k+1}(t)$ can be further replaced by the state equations in (18) and (19), which yields

$$\begin{aligned} \delta u_{k+1}(t) &= \delta u_k(t) - \Lambda C [-\delta \Psi_{k+1}(t) + f(x_d, t) - f(x_{k+1}, t) + B\delta u_{k+1}(t) - \omega_{k+1}(t)] \\ &\quad - \Lambda D \cdot {}_0D_t^\alpha \int_0^t [g(s, u_d) - g(s, u_{k+1})] ds + \Lambda \cdot {}_0D_t^\alpha v_{k+1}(t), \end{aligned} \quad (23)$$

where $\delta \Psi_{k+1}(t) = \Psi_d(t) - \Psi_{k+1}(t)$. Notice that

$$\begin{aligned} &{}_0D_t^\alpha \int_0^t [g(s, u_d) - g(s, u_{k+1})] ds \\ &= {}_0D_t^{\alpha-1} \frac{d}{dt} \int_0^t [g(s, u_d) - g(s, u_{k+1})] ds \\ &= {}_0D_t^{\alpha-1} [g(t, u_d) - g(t, u_{k+1})] \end{aligned} \quad (24)$$

according to (2), then applying (24) to reorganize (23) with respect to $\delta u_{k+1}(t)$ as

$$\begin{aligned} \delta u_{k+1}(t) = & (I + \Lambda CB)^{-1} \delta u_k(t) + (I + \Lambda CB)^{-1} \Lambda \cdot {}_0 D_t^\alpha v_{k+1}(t) \\ & - (I + \Lambda CB)^{-1} \Lambda C [-\delta \Psi_{k+1}(t) + f(x_d, t) - f(x_{k+1}, t) - \omega_{k+1}(t)] \\ & - (I + \Lambda CB)^{-1} \Lambda D \cdot {}_0 D_t^{\alpha-1} [g(t, u_d) - g(t, u_{k+1})]. \end{aligned} \tag{25}$$

Taking the λ -norm to both sides of (25) yields

$$\begin{aligned} & \|\delta u_{k+1}\|_\lambda = \sup_{t \in [0, T]} \left\{ e^{-\lambda t} \|\delta u_{k+1}(t)\|_\infty \right\} \\ \leq & \sup_{t \in [0, T]} \left\{ \|(I + \Lambda CB)^{-1}\|_\infty \cdot e^{-\lambda t} \|\delta u_k\|_\infty + \|(I + \Lambda CB)^{-1} \Lambda\|_\infty \cdot e^{-\lambda t} \|{}_0 D_t^\alpha v_{k+1}\|_\infty \right. \\ & + \|(I + \Lambda CB)^{-1} \Lambda C\|_\infty \cdot e^{-\lambda t} [\|\delta \Psi_{k+1}\|_\infty + \|f(x_d, t) - f(x_{k+1}, t)\|_\infty + \|\omega_{k+1}\|_\infty] \\ & \left. + \|(I + \Lambda CB)^{-1} \Lambda D\|_\infty \cdot e^{-\lambda t} \|{}_0 D_t^{\alpha-1} [g(t, u_d) - g(t, u_{k+1})]\|_\infty \right\} \\ \leq & \mu \|\delta u_k\|_\lambda + q [\|\delta \Psi_{k+1}\|_\lambda + \|f(x_d, \cdot) - f(x_{k+1}, \cdot)\|_\lambda + \|\omega_{k+1}\|_\lambda] \\ & + r \|{}_0 D_t^{\alpha-1} [g(\cdot, u_d) - g(\cdot, u_{k+1})]\|_\lambda + p \|{}_0 D_t^\alpha v_{k+1}\|_\lambda, \end{aligned} \tag{26}$$

where

$$\begin{aligned} \|(I + \Lambda CB)^{-1}\|_\infty &= \mu, \\ \|(I + \Lambda CB)^{-1} \Lambda\|_\infty &= p, \\ \|(I + \Lambda CB)^{-1} \Lambda C\|_\infty &= q, \\ \|(I + \Lambda CB)^{-1} \Lambda D\|_\infty &= r. \end{aligned}$$

For $\|f(x_d, \cdot) - f(x_{k+1}, \cdot)\|_\lambda$ and $\|g(\cdot, u_d) - g(\cdot, u_{k+1})\|_\lambda$, since f and g are Lipschitz continuous, then

$$\|f(x_d, \cdot) - f(x_{k+1}, \cdot)\|_\lambda \leq \sup_{0 \leq t \leq T} \{e^{-\lambda t} L_1 \cdot \|\delta x_{k+1}(t)\|_\infty\} = L_1 \|\delta x_{k+1}\|_\lambda, \tag{27}$$

$$\|g(\cdot, u_d) - g(\cdot, u_{k+1})\|_\lambda \leq \sup_{0 \leq t \leq T} \{e^{-\lambda t} L_2 \cdot \|\delta u_{k+1}(t)\|_\infty\} = L_2 \|\delta u_{k+1}\|_\lambda, \tag{28}$$

applying Lemma 1, (27) and (28) to (26) to eliminate f, g and the fractional operators, which yields

$$\begin{aligned} \left(1 - \frac{rL_2}{\lambda^{1-\alpha}}\right) \|\delta u_{k+1}\|_\lambda \leq & \mu \|\delta u_k\|_\lambda + qL_1 \|\delta x_{k+1}\|_\lambda \\ & + q [\|\delta \Psi_{k+1}\|_\lambda + \|\omega_{k+1}\|_\lambda] + \frac{p}{\lambda^{1-\alpha}} \|\dot{v}_{k+1}\|_\lambda, \end{aligned} \tag{29}$$

where

$$\|{}_0 D_t^{\alpha-1} [g(\cdot, u_d) - g(\cdot, u_{k+1})]\|_\lambda \leq \frac{1}{\lambda^{1-\alpha}} \|g(\cdot, u_d) - g(\cdot, u_{k+1})\|_\lambda \leq \frac{L_2}{\lambda^{1-\alpha}} \|\delta u_{k+1}\|_\lambda. \tag{30}$$

Step 2. In (29), the term $\|\delta x_{k+1}\|_\lambda$ needs to be substituted. For the Caputo-type fractional derivative with order $\alpha \in (0, 1)$, the following relationship holds:

$${}_t_0 D_t^{-\alpha} [{}_t_0 D_t^\alpha f(t)] = [{}_t_0 D_t^{-\alpha} {}_t_0 D_t^{\alpha-1}] \frac{d}{dt} f(t) = {}_t_0 D_t^{-1} \frac{d}{dt} f(t) = f(t) - f(t_0). \tag{31}$$

Thus, the state shift $\delta x_k(t) = x_d(t) - x_k(t)$ can be expressed as

$$\delta x_k(t) = \delta x_k(0) + {}_0 D_t^{-\alpha} {}_0 D_t^\alpha \delta x_k(t), \tag{32}$$

similarly to (23), ${}_0D_t^\alpha \delta x_k(t)$ in (32) can be replaced by the state equation:

$$\delta x_k(t) = \delta x_k(0) + {}_0D_t^{-\alpha} [-\delta \Psi_k(t) + f(x_d, t) - f(x_k, t) + B\delta u_k(t) - \omega_k(t)]. \quad (33)$$

Then, taking the ∞ -norm to (33) and applying Lemma 1 to eliminate the fractional integral yields

$$\begin{aligned} \|\delta x_k(t)\|_\infty &\leq \|\delta x_k(0)\|_\infty + \|{}_0D_t^{-\alpha} [B\delta u_k(t) - \delta \Psi_k(t) - \omega_k(t)]\|_\infty \\ &\quad + \left\| \int_0^t \frac{(t-s)^{\alpha-1}}{\Gamma(\alpha)} [f(x_d, s) - f(x_k, s)] ds \right\|_\infty \\ &\leq \|\delta x_k(0)\|_\infty + \frac{e^{\lambda t}}{\lambda^\alpha} [b\|\delta u_k\|_\lambda + \|\delta \Psi_k\|_\lambda + \|\omega_k\|_\lambda] \\ &\quad + \int_0^t \frac{L_1(t-s)^{\alpha-1}}{\Gamma(\alpha)} \|\delta x_k(s)\|_\infty ds, \end{aligned} \quad (34)$$

where $\|B\|_\infty = b$. Furthermore, since $\|\delta x_k(t)\|_\infty$ is nonnegative, and the first two terms on the right side of (34)

$$\|\delta x_k(0)\|_\infty + \frac{e^{\lambda t}}{\lambda^\alpha} [b\|\delta u_k\|_\lambda + \|\delta \Psi_k\|_\lambda + \|\omega_k\|_\lambda]$$

are nonnegative and nondecreasing with respect to t when $t \geq 0$, Lemma 2 can be applied to separate $\|\delta x_k(s)\|_\infty$ from the integral term, which yields:

$$\|\delta x_k(t)\|_\infty \leq E_\alpha(L_1 t^\alpha) \{ \|\delta x_k(0)\|_\infty + \frac{e^{\lambda t}}{\lambda^\alpha} [b\|\delta u_k\|_\lambda + \|\delta \Psi_k\|_\lambda + \|\omega_k\|_\lambda] \}. \quad (35)$$

To obtain the λ -norm of $\delta x_k(t)$, multiplying $e^{-\lambda t}$ to both sides of (35) yields

$$e^{-\lambda t} \|\delta x_k(t)\|_\infty \leq E_\alpha(L_1 t^\alpha) \{ e^{-\lambda t} \|\delta x_k(0)\|_\infty + \frac{1}{\lambda^\alpha} [b\|\delta u_k\|_\lambda + \|\delta \Psi_k\|_\lambda + \|\omega_k\|_\lambda] \}, \quad (36)$$

since $E_\alpha(L_1 t^\alpha)$ is nondecreasing on $[0, T]$, it is easy to see from (36) that

$$\begin{aligned} \|\delta x_k\|_\lambda &= \sup_{t \in [0, T]} \{ e^{-\lambda t} \|\delta x_k(t)\|_\infty \} \\ &\leq E_\alpha(L_1 T^\alpha) \|\delta x_k(0)\|_\infty + \frac{E_\alpha(L_1 T^\alpha)}{\lambda^\alpha} [b\|\delta u_k\|_\lambda + \|\delta \Psi_k\|_\lambda + \|\omega_k\|_\lambda]. \end{aligned} \quad (37)$$

Step 3. Based on the results of Steps 1 and 2, the convergence property of δu_k can ultimately be derived. Applying (37) to substitute $\|\delta x_{k+1}\|_\lambda$ in (29) yields

$$\begin{aligned} &\left(1 - \frac{rL_2}{\lambda^{1-\alpha}} - \frac{qbL_1E_\alpha(L_1T^\alpha)}{\lambda^\alpha}\right) \|\delta u_{k+1}\|_\lambda \\ &\leq \mu \|\delta u_k\|_\lambda + qL_1E_\alpha(L_1T^\alpha) \|\delta x_{k+1}(0)\|_\infty \\ &\quad + \left(q + \frac{qL_1E_\alpha(L_1T^\alpha)}{\lambda^\alpha}\right) \|\delta \Psi_{k+1}\|_\lambda \\ &\quad + \left(q + \frac{qL_1E_\alpha(L_1T^\alpha)}{\lambda^\alpha}\right) \|\omega_{k+1}\|_\lambda + \frac{p}{\lambda^{1-\alpha}} \|\dot{v}_{k+1}\|_\lambda, \end{aligned} \quad (38)$$

Note $O(\lambda^{-\alpha}) = \frac{qL_1E_\alpha(L_1T^\alpha)}{\lambda^\alpha}$, $O(\lambda^{\alpha-1}) = \frac{1}{\lambda^{1-\alpha}}$, then (38) can be rewritten as

$$\|\delta u_{k+1}\|_\lambda \leq \frac{\mu}{1 - bO(\lambda^{-\alpha}) - rL_2O(\lambda^{\alpha-1})} \|\delta u_k\|_\lambda + \varepsilon_{in,k+1} + \varepsilon_{ex,k+1}, \quad (39)$$

where ε_{in} and ε_{ex} are disturbance terms caused by internal initialization non-repetition and external channel noises:

$$\begin{aligned} \varepsilon_{in,k+1} = & \frac{qL_1E_\alpha(L_1T^\alpha)}{1 - bO(\lambda^{-\alpha}) - rL_2O(\lambda^{\alpha-1})} \|\delta x_{k+1}(0)\|_\infty \\ & + \frac{q + O(\lambda^{-\alpha})}{1 - bO(\lambda^{-\alpha}) - rL_2O(\lambda^{\alpha-1})} \|\delta\Psi_{k+1}\|_\lambda, \end{aligned} \tag{40}$$

$$\begin{aligned} \varepsilon_{ex,k+1} = & \frac{q + O(\lambda^{-\alpha})}{1 - bO(\lambda^{-\alpha}) - rL_2O(\lambda^{\alpha-1})} \|\omega_{k+1}\|_\lambda \\ & + \frac{pO(\lambda^{\alpha-1})}{1 - bO(\lambda^{-\alpha}) - rL_2O(\lambda^{\alpha-1})} \|\dot{v}_{k+1}\|_\lambda. \end{aligned} \tag{41}$$

Here, $\|\delta x_{k+1}(0)\|_\infty$, $\|\omega_{k+1}\|_\lambda$ and $\|\dot{v}_{k+1}\|_\lambda$ are bounded according to Assumptions (A) and (C). In addition, it follows from Assumption (B) and (4) that

$$\begin{aligned} \|\delta\Psi_{k+1}\|_\lambda &= \sup_{t \in [0, T]} \{e^{-\lambda t} \|\delta\Psi_{k+1}(t)\|_\infty\} \\ &\leq \sup_{t \in [0, T]} \int_{t_0}^0 \frac{e^{-\lambda t}(t-s)^{-\alpha}}{\Gamma(1-\alpha)} \left\| \frac{d}{ds} [\phi_d(s) - \phi_{k+1}(s)] \right\|_\infty ds \\ &\leq M \cdot \sup_{t \in [0, T]} \int_{t_0}^0 \frac{(t-s)^{-\alpha}}{\Gamma(1-\alpha)} ds \\ &= \frac{M}{\Gamma(2-\alpha)} \sup_{t \in [0, T]} [(t-t_0)^{1-\alpha} - t^{1-\alpha}] \\ &\leq \frac{M}{\Gamma(2-\alpha)} (T-t_0)^{1-\alpha}, \end{aligned} \tag{42}$$

which means that $\|\delta\Psi_{k+1}\|_\lambda$ is bounded as well. Since $O(\lambda^{-\alpha})$ and $O(\lambda^{\alpha-1})$ can be arbitrarily small when λ is large enough, if μ is strictly less than 1, an appropriate $\lambda > 0$ can always be found so that

$$\frac{\mu}{1 - bO(\lambda^{-\alpha}) - rL_2O(\lambda^{\alpha-1})} \leq \mu' < 1, \tag{43}$$

where μ' is a constant. Therefore, δu_k is bounded according to Lemma 3 such that $\sup_{k \in \mathbb{N}} \|\delta u_k\|_\lambda \leq \varepsilon_u$ for some $\varepsilon_u > 0$. Additionally, if the following assumption holds,

$$(D) \quad \lim_{k \rightarrow \infty} x_k(0) = x_d(0); \lim_{k \rightarrow \infty} \phi_k(t) = \phi_d(t), \text{ where } t \in [t_0, 0]; \lim_{k \rightarrow \infty} \omega_k(t) = \lim_{k \rightarrow \infty} v_k(t) = 0, \text{ where } t \in [0, T].$$

then $\lim_{k \rightarrow \infty} \|\delta u_k\|_\lambda = 0$ as $\lim_{k \rightarrow \infty} (\varepsilon_{in,k} + \varepsilon_{ex,k}) = 0$.

Step 4. The convergence results δx_k and e_k are derived from the boundedness of $\|\delta u_k\|_\lambda$. First, it is obvious that the following inequality holds according to Definition 3:

$$\|\delta u_k\|_\lambda \leq \sup_{t \in [0, T]} \|\delta u_k(t)\|_\infty \leq e^{\lambda T} \|\delta u_k\|_\lambda, \tag{44}$$

which indicates that the boundedness and convergence properties of $\sup_{t \in [0, T]} \|\delta u_k(t)\|_\infty$ are exactly the same as $\|\delta u_k\|_\lambda$. Furthermore, it follows from (37) that δx_k is bounded, i.e., $\sup_{k \in \mathbb{N}, t \in [0, T]} \|\delta x_k(t)\|_\infty \leq \varepsilon_x$ for some $\varepsilon_x > 0$, since $\|\delta x_k(0)\|_\infty$, $\|\delta u_k\|_\infty$, $\|\delta\Psi_k\|_\infty$, and $\|\omega_k\|_\infty$ are all bounded according to Assumptions (A-C). In addition, if Assumption (D) holds, then $\lim_{k \rightarrow \infty} \sup_{t \in [0, T]} \|\delta x_k(t)\|_\infty = 0$.

Finally, for the output error e_k , it follows from the output equation of (19) that

$$e_k(t) = C\delta x_k(t) + D \int_0^t [g(s, u_d) - g(s, u_k)]ds - v_k(t), \tag{45}$$

taking the ∞ -norm to both sides of (45) yields

$$\begin{aligned} \| e_k(t) \|_\infty &\leq c \| \delta x_k(t) \|_\infty + d \int_0^t \| g(s, u_d) - g(s, u_k) \|_\infty ds + \| v_k(t) \|_\infty \\ &\leq c \| \delta x_k(t) \|_\infty + d \int_0^t L_2 \| \delta u_k(t) \|_\infty ds + \| v_k(t) \|_\infty \\ &\leq c \| \delta x_k(t) \|_\infty + dTL_2 \sup_{t \in [0, T]} \| \delta u_k(t) \|_\infty + \| v_k(t) \|_\infty, \end{aligned} \tag{46}$$

where $\| C \|_\infty = c$, $\| D \|_\infty = d$. Since $\| v_k(t) \|_\infty$ is bounded according to Assumption (C), the boundedness and convergence conditions of e_k is the same as that of δu_k and δx_k .

Theorem 1 and Remarks 1 and 2 can be summarized from the derivation.

Theorem 1. For the iterative system (19), given an arbitrary bounded initial input $u_0(t)$, ($t \in [0, T]$). The close-loop D^α -type updating law (20) is adopted to track the reference system (18). If

$$\| (I + \Lambda CB)^{-1} \|_\infty < 1, \tag{47}$$

then the following conclusions hold:

- (i) If the assumptions (A-C) hold, then there are some positive constant ϵ_u , ϵ_x and ϵ_e , such that $\sup_{k \in \mathbb{N}, t \in [0, T]} \| \delta u_k(t) \|_\infty \leq \epsilon_u$, $\sup_{k \in \mathbb{N}, t \in [0, T]} \| \delta x_k(t) \|_\infty \leq \epsilon_x$, $\sup_{k \in \mathbb{N}, t \in [0, T]} \| e_k(t) \|_\infty \leq \epsilon_e$
- (ii) If the assumption (D) additionally holds, then $\lim_{k \rightarrow \infty} \sup_{t \in [0, T]} \| \delta u_k(t) \|_\infty = \lim_{k \rightarrow \infty} \sup_{t \in [0, T]} \| \delta x_k(t) \|_\infty = \lim_{k \rightarrow \infty} \sup_{t \in [0, T]} \| e_k(t) \|_\infty = 0$.

Conclusion (i) in Theorem 1 indicates that under Assumptions (A-C), the tracking errors remain bounded during the iteration process. Furthermore, the size of the final tracking errors and its algorithm factors can be theoretically analyzed.

Remark 1. It can be seen from the derivation process that, without considering the external disturbances, the tracking error level depends on the degree of shift of ϕ_k compared to ϕ_d . Taking δu_k as an example, the inequality (39) becomes

$$\| \delta u_{k+1} \|_\lambda \leq \Theta_\lambda \| \delta u_k \|_\lambda + \epsilon_{in, k+1} \tag{48}$$

if $\epsilon_{ex, k+1} = 0$, where $\Theta_\lambda = \frac{\mu}{1 - bO(\lambda^{-\alpha}) - rL_2O(\lambda^{\alpha-1})}$. If $\Theta_\lambda < 1$, $\| \delta u \|_\lambda$ will decrease until $\Theta_\lambda \| \delta u_k \|_\lambda + \epsilon_{in, k+1} \geq \| \delta u_k \|_\lambda$, i.e., $\| \delta u_k \|_\lambda \leq \frac{\epsilon_{in, k+1}}{1 - \Theta_\lambda}$ for some iteration index k , then $\| \delta u \|_\lambda$ may stop converging and remain at the level of $\frac{\epsilon_{in, k+1}}{1 - \Theta_\lambda}$, which is proportional to $\epsilon_{in, k+1}$. This result is adequate for most tracking problems. In addition, since $\epsilon_{in, k}$ is proportional to $\| \delta x_k(0) \|_\infty$ and $\| \delta \Psi_k \|_\lambda$, and ultimately determined by $\delta \phi_k$ according to (40), the tracking performance can be improved by reducing the initialization shift. In this regard, the preconditioning based initialization strategy [28] is noteworthy, as it can eliminate initial shift and reduce $\| \delta \Psi_k \|_\lambda$.

It can be seen from Remark 1 that the tracking performance of the iterative system can always be improved by controlling the disturbance terms, especially $\delta \phi_k$. The perfect tracking is achieved when the disturbance terms strictly converge to zero according to conclusion (ii). The corresponding strategies will be discussed in detail in Section 4.2. Finally, the following Remark 2 provides some explanations on the system assumptions and the selection of ILC updating law.

Remark 2. In Assumptions (B) and (C), the specifications about $\delta\dot{\phi}_k(t)$ and $\dot{v}_k(t)$ are related to the definition of the Caputo-type fractional derivative. The boundedness of the first-order derivative is necessary to ensure the boundedness of other signals in the system, as the derivative is performed before the $(1 - \alpha)_{th}$ -order integral. Specifically, for the output channel noise $v_k(t)$, the boundedness of $\dot{v}_k(t)$ is crucial for obtaining a bounded output signal u_k , since it is required to calculate the fractional derivative of the tracking error e_k in the updating law (20). If $v_k(t)$ does not meet this assumption, it is necessary to avoid using derivative operators in the ILC updating law to prevent amplifying noise.

4.2. Perfect Tracking with Initialization Learning Algorithm

As discussed in Section 3, the initialization path directly affects the dynamic characteristics of fractional-order systems. In applied disciplines such as secondary battery [36] and viscoelasticity [37], this historical hereditary effect can usually not be neglected. Identification and fitting of history function is crucial for improving system performance [21]. In this section, the ILC tracking problem is considered in conjunction with the optimization of ϕ_k , and a novel initialization learning algorithm is proposed to achieve perfect tracking performance.

The idea of initialization learning is inspired by the well-known initial state learning strategy [38]; the latter uses the initial output error for iteration and thereby gradually converging $x_k(0)$ to the optimal $x_d(0)$. Since the history function ϕ can be viewed as an extension of the state variable x on interval $[t_0, 0)$, the learning algorithm for $x(0)$ can be applied throughout the initialization stage. To achieve this target, the definitions of history function and initial state are unified into the following form:

$$\tilde{\phi}(t) = \begin{cases} \phi(t), t \in [t_0, 0), \\ x(0), t = 0, \end{cases} \quad (49)$$

where $\tilde{\phi}(t) : [t_0, 0] \rightarrow \mathbb{R}^n$ is called the complete history function. In addition, the system output on interval $[t_0, 0]$ is noted as \tilde{y} .

In order to obtain the perfect convergence condition, the non-repetitive channel disturbances ω and ν are no longer considered here. Supposing that there is no external input u on $[t_0, 0]$, or the input–output channel matrix $D = 0$. In both situations, the output error can be expressed as

$$\tilde{e}_k(t) = \tilde{y}_d(t) - \tilde{y}_k(t) = C[\tilde{\phi}_d(t) - \tilde{\phi}_k(t)] = C\delta\tilde{\phi}_k(t), \quad (50)$$

where $t \in [t_0, 0]$, $\delta\tilde{\phi}_k(t) = \tilde{\phi}_d(t) - \tilde{\phi}_k(t)$ denotes the tracking error of $\tilde{\phi}_k(t)$. Then, for an ideal reference (ϕ_d, u_d, y_d) , if the system output is measurable, Lemma 4 is proposed to eliminate the initialization shift and thereby improve the ILC performance.

Lemma 4. For the iterative system (17) and reference system (18), suppose that $D = 0$. Given a bounded and piecewise smooth $\tilde{\phi}_d(t)$ and an arbitrary bounded and piecewise smooth initial $\tilde{\phi}_0(t)$, for $k \in \mathbb{N}$, the initialization learning strategy

$$\tilde{\phi}_{k+1}(t) = \tilde{\phi}_k(t) + \Upsilon\tilde{e}_k(t) \quad (51)$$

is adopted for iteration, where Υ is the learning operator. If $\|I - \Upsilon C\|_\infty < 1$, then

$$\lim_{k \rightarrow \infty} \|\delta x_k(0)\|_\infty = \lim_{k \rightarrow \infty} \|\delta \Psi_k\|_\lambda = 0.$$

Proof. It follows from (51) that

$$\begin{aligned} \delta\tilde{\phi}_{k+1}(t) &= \delta\tilde{\phi}_k(t) - [\tilde{\phi}_{k+1}(t) - \tilde{\phi}_k(t)] \\ &= \delta\tilde{\phi}_k(t) - Y\tilde{e}_k(t) \\ &= (I - YC)\delta\tilde{\phi}_k(t), \end{aligned} \tag{52}$$

where $t \in [t_0, 0]$. When $t = 0$, $\delta\tilde{\phi}_k(0) = \delta x_k(0)$ since $\lim_{t \rightarrow 0^-} \phi_k(t) = x_k(0)$, then taking the ∞ -norm to both sides of (52) yields

$$\| \delta x_{k+1}(0) \|_\infty \leq \| I - YC \|_\infty \| \delta x_k(0) \|_\infty, \tag{53}$$

thus $\lim_{k \rightarrow \infty} \| \delta x_k(0) \|_\infty = 0$ according to the condition $\| I - YC \|_\infty < 1$.

Similarly, for $t \in [t_0, 0)$, taking the derivative with respect to t to both sides of (52), which yields

$$\delta\dot{\phi}_{k+1}(t) = (I - YC)\delta\dot{\phi}_k(t), \tag{54}$$

then applying the ∞ -norm yields

$$\| \delta\dot{\phi}_{k+1}(t) \|_\infty \leq \| I - YC \|_\infty \| \delta\dot{\phi}_k(t) \|_\infty, \tag{55}$$

thus $\lim_{k \rightarrow \infty} \| \delta\dot{\phi}_k(t) \|_\infty = 0$ if $\| I - YC \|_\infty < 1$. Finally, it follows from (42) that

$$\begin{aligned} \| \delta\Psi_k \|_\lambda &\leq \sup_{t \in [0, T]} \int_{t_0}^0 \frac{e^{-\lambda t}(t-s)^{-\alpha}}{\Gamma(1-\alpha)} \| \delta\dot{\phi}_k(s) \|_\infty ds \\ &\leq \sup_{t \in [0, T]} \int_{t_0}^0 \frac{(t-s)^{-\alpha}}{\Gamma(1-\alpha)} ds \cdot \sup_{t \in [t_0, 0)} \| \delta\dot{\phi}_k(t) \|_\infty \\ &\leq \frac{(T-t_0)^{1-\alpha}}{\Gamma(2-\alpha)} \cdot \sup_{t \in [t_0, 0)} \| \delta\dot{\phi}_k(t) \|_\infty, \end{aligned} \tag{56}$$

which means that $\lim_{k \rightarrow \infty} \| \delta\Psi_k \|_\lambda = 0$ as well. \square

Returning to the inequality (39), since $\varepsilon_{ex,k+1}$ no longer exists and $\lim_{k \rightarrow \infty} \varepsilon_{in,k+1} = 0$ according to Lemma 4, then it follows from Lemma 3 that $\| \delta u_k(t) \|$, $\| \delta x_k(t) \|$ and $\| e_k(t) \|$ all converge to 0 as k grows. This indicates that, without considering external disturbances, the initialization learning strategy proposed in Lemma 4 can gradually eliminate the distortion of system dynamics caused by initialization and initial state shift, thereby achieving ideal tracking performance for the ILC scheme proposed in Section 4.1. Finally, the following Theorem 2 can be concluded.

Theorem 2. For the iterative system (17) and reference system (18), suppose that $D = 0$. Given an arbitrary bounded initial input $u_0(t)$ ($t \in [0, T]$) and an arbitrary bounded and piecewise smooth initial $\tilde{\phi}_0(t)$ ($t \in [t_0, 0]$); for $k \in \mathbb{N}$, the following close-loop D^α -type ILC scheme with initialization learning is adopted:

$$\begin{cases} u_{k+1}(t) = u_k(t) + \Lambda \cdot {}_0D_t^\alpha e_{k+1}(t), \\ \tilde{\phi}_{k+1}(t) = \tilde{\phi}_k(t) + Y\tilde{e}_k(t). \end{cases} \tag{57}$$

If

$$\| (I + \Lambda CB)^{-1} \|_\infty < 1, \| I - YC \|_\infty < 1, \tag{58}$$

then the following conclusion holds:

$$\lim_{k \rightarrow \infty} \sup_{t \in [0, T]} \| \delta u_k(t) \|_\infty = \lim_{k \rightarrow \infty} \sup_{t \in [0, T]} \| \delta x_k(t) \|_\infty = \lim_{k \rightarrow \infty} \sup_{t \in [0, T]} \| e_k(t) \|_\infty = 0.$$

5. Numerical Examples

5.1. Example 1

A fractional capacitor is a key element in fractional order models of electrochemistry [39,40] and batteries [41]. Different from integer order capacitors, the voltage and current of a fractional capacitor exhibit a relationship of fractional derivative, and its constitutive equation is

$${}_0^C \mathcal{D}_t^\alpha u(t) = Ci(t), \quad (59)$$

where $\alpha \in (0, 1)$ denotes the fractional order, $u(t)$ is the voltage, $i(t)$ is the current, C is a constant. A fractional capacitor is also called a constant phase element (CPE), as the phase of the impedance of fractional capacitor only depends on the the fractional exponent α from the view of frequency domain [29]. The initialized fractional operator \mathcal{D} is applied here because the CPE is memorial and its performance is affected by the history voltage curve. In charging and discharging experiments related to CPE, it is usually necessary to resting the equipment to eliminate the polarization effect [42], or apply appropriate initialization stimulus to obtain the required system performance.

In this example, the voltage tracking problem of the CPE is considered, where the reference $u_d(t) = 12t^2(1-t)$ ($t \in [0, 1]$), the order α is set to be 0.5, $C = 1$, and the current i is chosen as the control input. To achieve this target, the close-loop D^α -type updating law (20) is applied and the operator Λ is selected as 0.5, which conforms to the convergence condition (47). The initial input current is set as $i_0(t) = 0$, $t \in [0, 1]$. The simulations are carried out in the environment of MATLAB/SIMULINK, where a number of mature open-source toolboxes [43] on fractional calculus are available. The fractional operator is implemented in the frequency domain and packaged as filter modules by adopting integer-order fitting algorithms. The objective fractional order iterative system can be easily established with the help of some other commonly used modules.

Suppose that the CPE is initialized on $[-2, 0)$, the history voltage trajectory is symbolled as ϕ_k during the iterations. The following two initialization scenarios are concerned:

- (1) For a constant reference history function $\phi_d(0) = 0$ ($t \in [-2, 0)$), the initialization trajectory $\phi_k(t)$ is disturbed by a iteration-varying $\delta\phi_k(t)$, such that $\phi_k(t) = \phi_d(t) + \delta\phi_k(t) = \delta\phi_k(t)$, and the initial shift $\delta u_k(0) = \lim_{t \rightarrow 0^-} \delta\phi_k(t)$. Then, are the tracking errors of u_k and i_k bounded? What factors are related to the size of the errors?
- (2) If the reference history function is set as a sinusoidal excitation signal $\phi_d(t) = 0.2 \sin(\frac{3\pi t}{2} + \pi)$, while the initial initialization path $\phi_0(t) = 0.2 \sin(\frac{5\pi t}{4} + \frac{\pi}{2})$ deviates from $\phi_d(t)$ and further causes a significant initial shift $\delta u_0(0) = 0.2$. Then, can the initialization learning strategy (51) be applied to achieve the perfect tracking performance of ϕ_k , u_k and i_k ?

For Problem (1), the disturbed $\phi_k(t)$ is illustrated as follows. First, since ϕ_k needs to be piecewise differentiable according to the Caputo definition, $\frac{d\phi_k(t)}{dt}$ is assumed to be uniformly distributed on $[-L, L]$, which can be generated by the Simulink block "Uniform Random Number". The sample time is set as 0.01s. Then, $\phi_k(t)$ is obtained by filtering $\frac{d\phi_k(t)}{dt}$ through an integrator. Obviously, $\phi_k(t)$ and $\delta u_k(0)$ are both bounded. Figure 1 shows the generation process of disturbed history function $\phi_k(t)$.

Set $L = 0, 1$, and 2 , respectively, and perform 30 iterations ($L = 0$ means that $\delta\phi_k(t) = \delta u_k(0) = 0$, $\phi_k(t) = \phi_d(t)$); the results are shown in Figure 2. Therein, the reference input i_d is the current trajectory corresponding to u_d under ideal initialization condition $\phi_d(t) = 0$ ($t \in [-2, 0)$). From Figure 2a,c, it can be observed that the tracking error of u and i remain bounded, and the convergence process are presented in Figure 2b,d. It should be noted that i_k fluctuates significantly near $t = 0$ due to the iteration-varying ϕ_k and $u_k(0)$ [28]. Thus, the root-mean-square (RMS) value of $\delta i_k(t)$ is adopted to measure the input performance on the entire $[0, 1]$, and the maximum absolute value of $\delta u_k(t)$ is applied to evaluate the output performance.

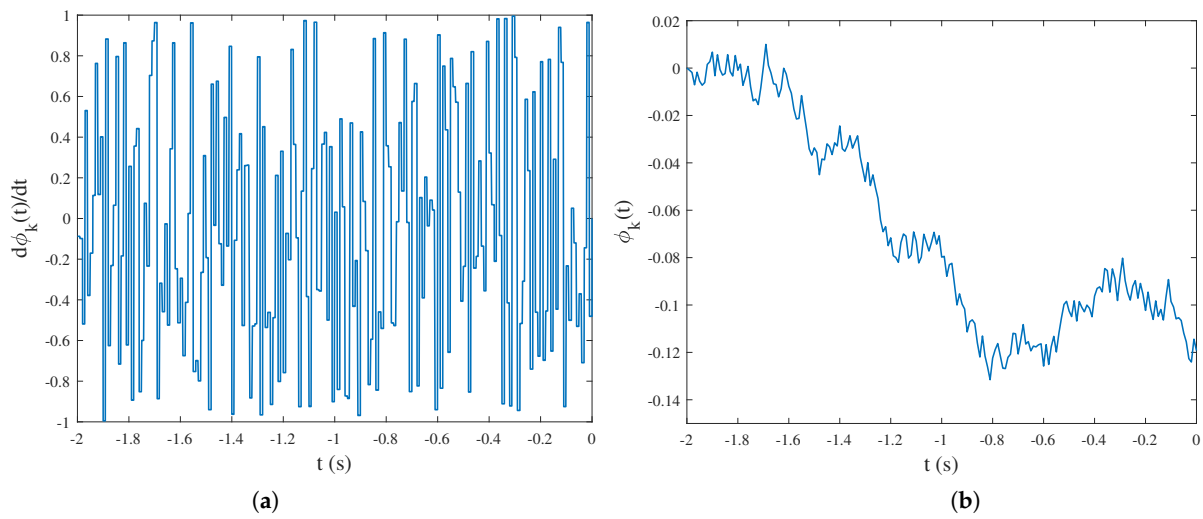


Figure 1. Generation of the disturbance signals: (a) The first-order derivative signal of $\phi_k(t)$ on $[-2, 0)$, where $L = 1$, $t_s = 0.01s$. (b) $\phi_k(t)$ is generated by integrating the derivative signal, where $\phi_k(-2) = 0$, $\phi_k(0-) = x_k(0)$.

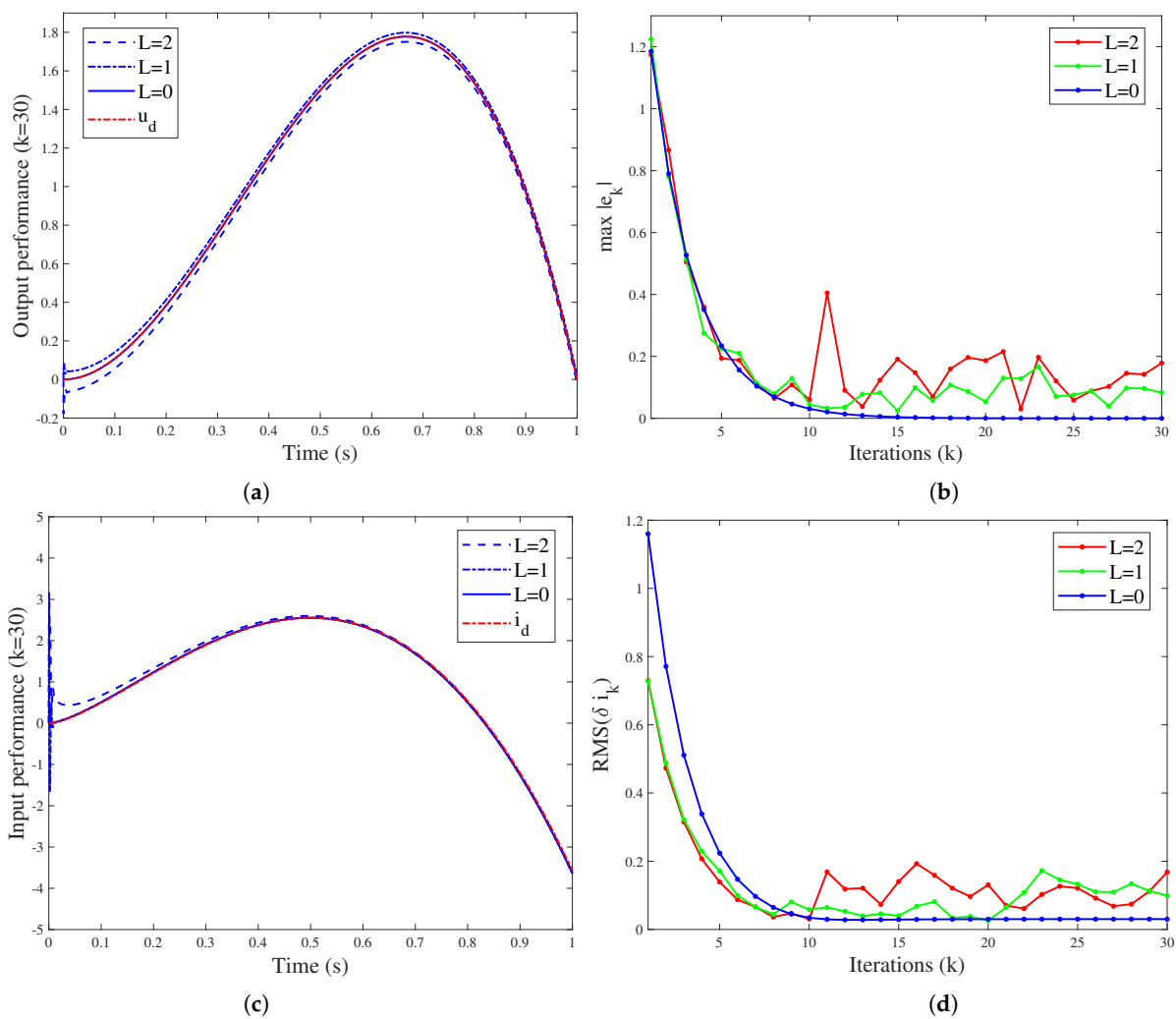


Figure 2. System performance for different history function fluctuations (L): (a) The output performance after 30 iterations. (b) Convergence of the maximum tracking error $\max_{t \in [0,1]} |e_k(t)|$. (c) The input performance after 30 iterations. (d) Convergence of RMS value of the input error $\delta i_k(t)$ on $[0, 1]$.

It is seen from Figure 2b,d that after about 15 iterations, the tracking error stops converging and fluctuates due to random initialization path. To clarify the impact of L on system performance, the values of $\max_{t \in [0,1]} |e_k(t)|$ and $RMS_{t \in [0,1]}(\delta i_k(t))$ for the 16th–30th iterations are recorded, and then their RMS values are calculated, respectively. The results are stated in Table 1. The error level is positively correlated with the size of L . Since the size of L reflects the fluctuation degree of $\delta\phi_k(t)$ and $u_k(0)$, it can be concluded that the ILC performance depends on the shift degree of the initialization path, which has been theoretically illustrated in Remark 1.

Table 1. The RMS value of the tracking errors for the 16th–30th iterations.

Size of L	2	1	0
$RMS_{16 \leq k \leq 30}(\max_{t \in [0,1]} e_k(t))$	0.1463	0.0972	0.0010
$RMS_{16 \leq k \leq 30}(RMS_{t \in [0,1]}(\delta i_k(t)))$	0.1191	0.1044	0.0301

Furthermore, the initialization problem (2) is considered. Obviously, if the initial ϕ_0 is not processed, the shift of initialization and initial value will break the convergence of the system. To obtain the perfect tracking performance, the close-loop D^α -type ILC scheme with initialization learning (57) is applied, where $\Lambda = 0.5$, the learning Y is set as 0.2, which conforms to the convergence condition (58). The initialization learning is applied on $[-2, 0]$, while the ILC algorithm is performed on $[0, 2]$.

Without considering other disturbances, we performed 100 iterations, and the results are shown in Figure 3. Therein, Figure 3a–c demonstrate the trajectory of u_k , i_k and ϕ_k through the iterations, and Figure 3d gives the changes in the tracking errors. It can be concluded that after 100 iterations, u_{100} , i_{100} and ϕ_{100} can accurately track the reference trajectories. The convergence speed of i_k is slower, which is caused by the initial shift and evolution of the initialization path.

As a comparative experiment, another 100 iterations are carried out without using the initialization learning strategy (51), and the results are displayed together with the u_{100} and i_{100} of Figure 3, as shown in Figure 4. Obviously, the output voltage fluctuates at the initial moment without initialization learning, which is not desirable in practice. The situation with the input current is even worse, and a significant tracking error can be observed. On the contrary, when applying the ILC scheme (57), the system maintains good tracking performance, which proves the superiority of the proposed initialization learning strategy.

For ILC problems with initialization learning, it is significant to identify and optimize the initialization path ϕ . This issue is theoretically challenging, since ϕ is infinite dimensional, and the analytical relationship between ϕ and its response signal Ψ is relatively complex. In this regard, some discretization based data-driven strategies are notable [44–46], as it is difficult to apply the analytical methods. In addition, for more complex initialized fractional order systems, it may be difficult to calculate ϕ_d and u_d . Nevertheless, the proposed initialization learning algorithm still has potential value, since the design of ϕ_d depends on various factors such as physical accessibility, operating costs, and system performance. For example, when ϕ_0 causes an initial shift and leads to an excessive tracking error, ϕ_d can be designed as an achievable initialization path which satisfies $\phi_d(0_-) = y_d(0)$. The initial shift can be eliminated by applying the initialization learning.

5.2. Example 2

In this section, a more complex system structure, which contains nonlinearity, output equation and channel disturbances, is considered:

$$\begin{cases} {}^C_0\mathcal{D}_t^{0.85}x_1(t) = x_2(t) + 0.5u(t) + \omega_1(t), \\ {}^C_0\mathcal{D}_t^{0.85}x_2(t) = |x_1(t)| + 0.8x_2^{0.6}(t) + u(t) + \omega_2(t), \\ y(t) = x_1(t) + 0.2 \int_0^t e^s u(s) ds + v(t), \end{cases} \quad (60)$$

where x_1 and x_2 are state variables, u is the control input, y is the output, ω and ν are disturbance signals. The proposed ILC strategy is applied to track the reference $y_d(t) = 12t^2(1-t)$, where $t \in [0, 1]$. Under the initial input $u_0(t) = 0, (t \in [0, 1])$, the close-loop D^α -type ILC updating law (20) is adopted, where the learning gain Λ is set to be 0.5 to satisfy the convergence conditions. Suppose that ${}^C_0D_t^{0.85}x_1(t)$ is initialized by a history function $\phi(t)$ on $[-2, 0)$; similarly to Example 1, the following two initialization scenarios are considered: (1) $\phi_k(t)$ is iteration-varying within a bounded range; and (2) the initial $\phi_0(t)$ deviates from ϕ_d and needs to be addressed.

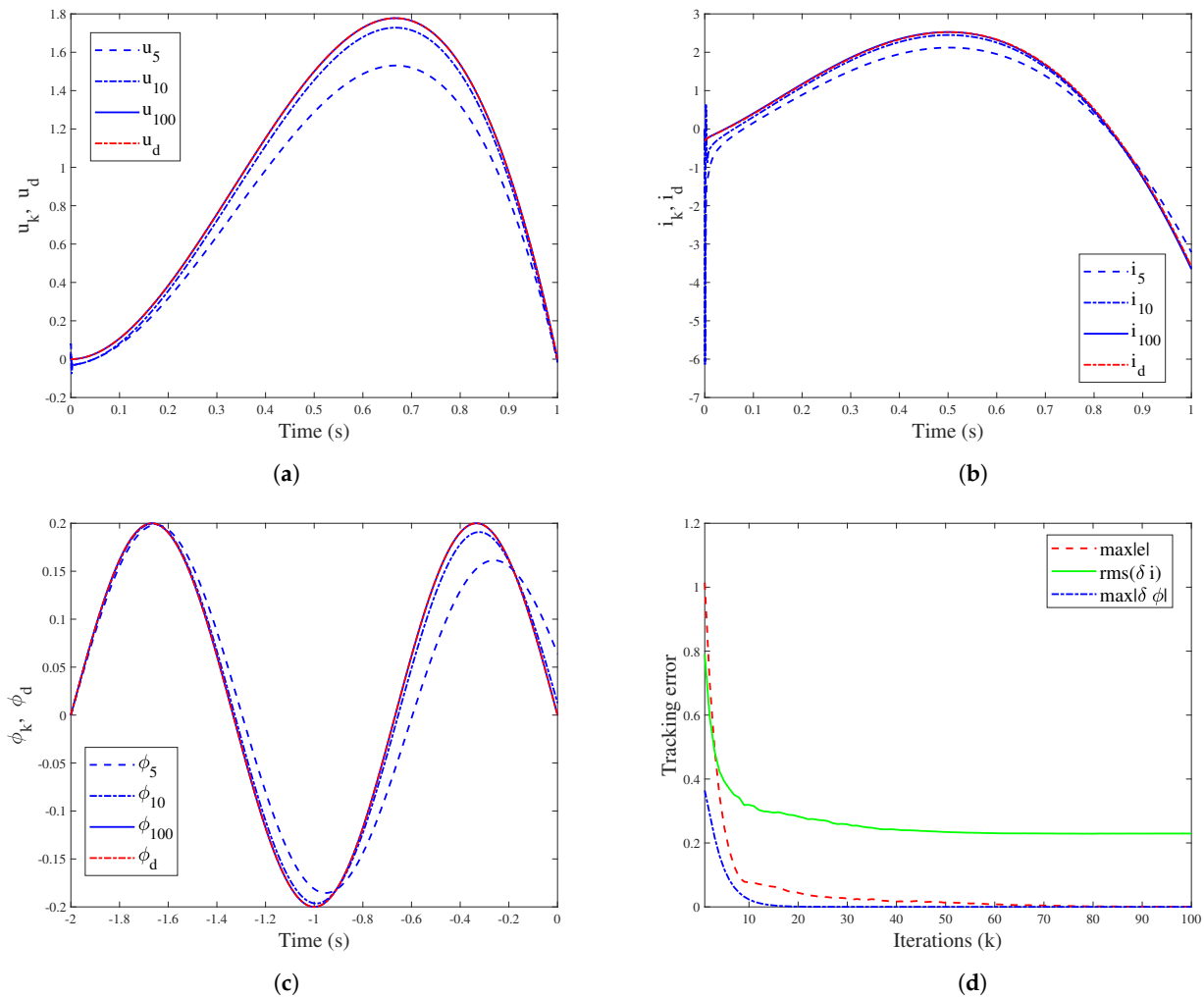


Figure 3. System performance when applying the initialization learning strategy: (a) The tracking performance of u_k . (b) The tracking performance of i_k . (c) The tracking performance of ϕ_k . (d) Convergence of the tracking errors δu , δi , and $\delta \phi$ during the iterations.

First, for scenario (1), suppose that $\phi_d(t) = 0 (t \in [-2, 0))$, $\phi_k(t)$ is disturbed by a iteration-varying $\delta\phi_k(t)$. In order to eliminate interference from other non-repetitive factors, $\delta x_{1,k}(0)$ is set to be 0, and $\omega_1(t) = \omega_2(t) = \nu(t) = 0$ on $[0, 1]$. The generation of $\delta\phi_k(t)$ is the same as that shown in Figure 1, and the sample time is set as 0.001s here. To clarify the impact of $\delta\phi_k(t)$ on system performance, 50 iterations are performed, respectively, for $L = 20, 10, 0$, and the simulation results are shown in Figure 5. It can be seen that the tracking error keeps bounded. Similarly, recording the maximum absolute error $\max_{t \in [0, 1]} |e_k(t)|$ for the 16th–50th iterations and then calculating their RMS values, the results are $RMS_{L=20}(e_{16 \leq k \leq 50}) = 0.0657$, $RMS_{L=10}(e_{16 \leq k \leq 50}) = 0.0363$, $RMS_{L=0}(e_{16 \leq k \leq 50}) = 0.0011$. Thus, it is concluded that the average tracking error level is positively correlated with the shift degree of the initialization path.

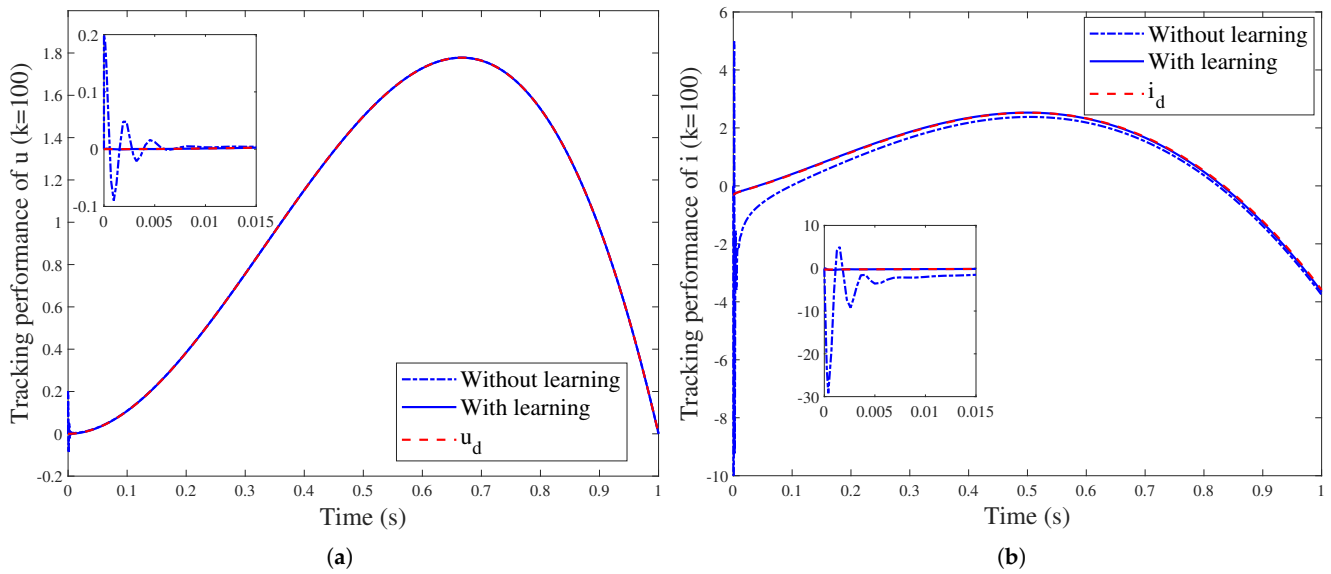


Figure 4. System performance with/without initialization learning ($k = 100$): (a) The tracking performance of u_{100} and the fluctuation at the initial moment. (b) The tracking performance of i_{100} and the fluctuation phenomenon.

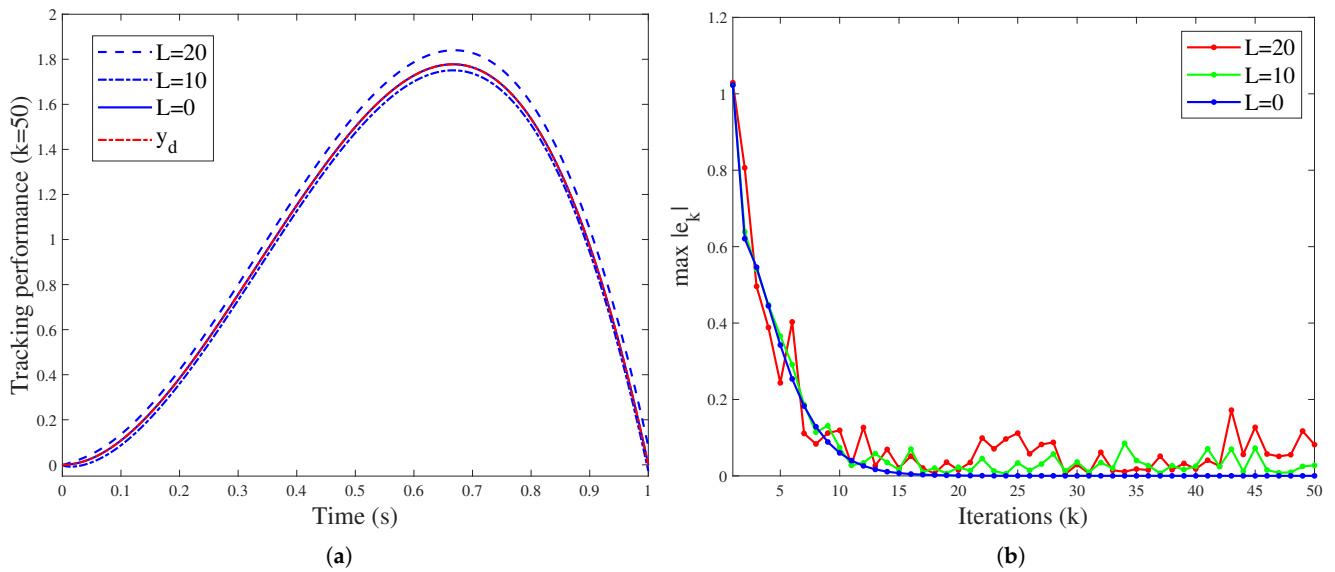


Figure 5. System performance for different history function fluctuations (L): (a) The tracking performance after 50 iterations. (b) Convergence of the maximum tracking error $\max_{t \in [0,1]} |e_k(t)|$.

Second, the effects of initial shift and channel disturbances on ILC performance is further investigated. Based on the first step, assuming that $x_{1,k}(0) = \phi_k(0_-)$, $\omega_{1,k}$, $\omega_{2,k}$ and ν_k are generated similarly as ϕ_k . For $L = 4, 2, 0$, perform 50 iterations, and the results can be seen in Figure 6. The RMS values of $\max_{t \in [0,1]} |e_k(t)|$ for the 16th–50th iterations are 0.2992 ($L = 4$), 0.1606 ($L = 2$) and 0.0011 ($L = 0$), respectively. Combined with Figures 5b and 6b, it can be concluded that the superposition of non-repetitive factors leads to an increase in average tracking error, but its overall level is still positively correlated with the amplitude ($x_{1,k}(0)$, ω_k) and fluctuation level ($\delta\phi_k$, ν_k) of the disturbances. This conclusion is consistent with the theoretical results in Section 4.

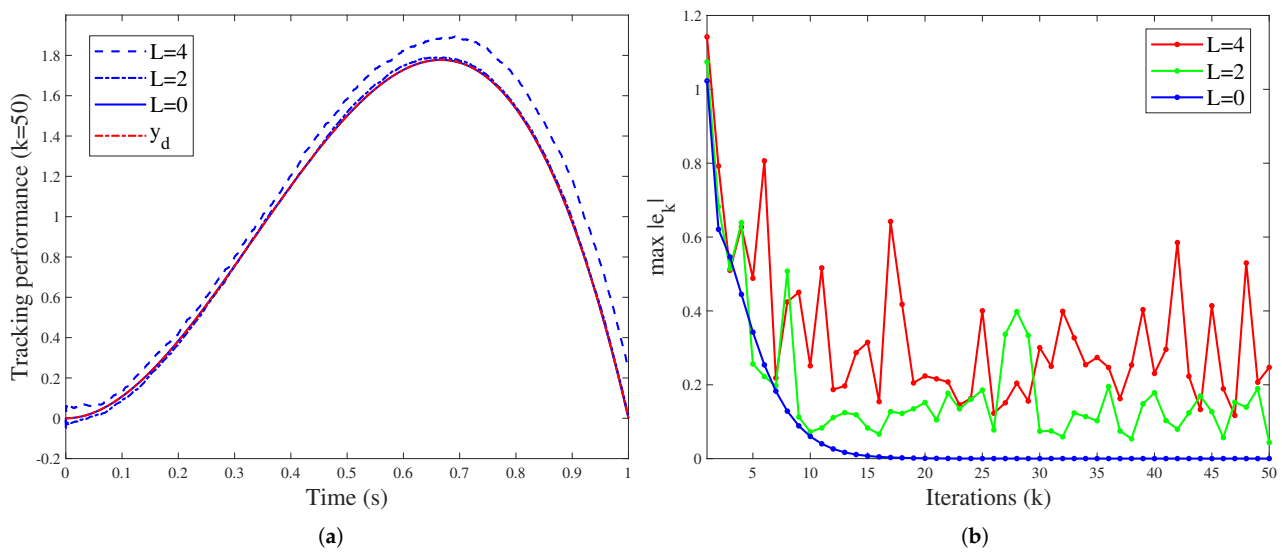


Figure 6. System performance for different history function fluctuations, initial shifts, and channel disturbances: (a) The tracking performance after 50 iterations. (b) Convergence of the maximum tracking error $\max_{t \in [0,1]} |e_k(t)|$.

Third, for the initialization scenario (2), suppose that $\omega_1(t) = \omega_2(t) = v(t) = 0$ on $[0, 1]$, the initial initialization path $\phi_0(t) = 0.2 \sin(\frac{5\pi t}{4} + \frac{\pi}{2})$, where $t \in [-2, 0)$, $\phi_0(0_-) = x_{1,0}(0) = 0.2$. Appropriate adjustment of ϕ_0 is necessary to eliminate the initial shift. Therefore, the reference initialization path is set to be $\phi_d(t) = 0.2 \sin(\frac{3\pi t}{2} + \pi)$ ($t \in [-2, 0)$), such that $x_{1,d}(0) = \lim_{t \rightarrow 0_-} \phi_d(t) = 0$. To apply the initialization learning algorithm, the system is assumed to have no control inputs on $[-2, 0]$. Then, we adopt the learning law $\hat{\phi}_{k+1}(t) = \hat{\phi}_k(t) + 0.2\tilde{e}_k(t)$ and perform 50 iterations; the results are presented in Figure 7. It can be seen that the initial error is gradually eliminated, and the system output achieves perfect tracking of the reference trajectory. As a comparison, Figure 7 also shows the tracking performance after 50 iterations without using initialization learning. Obvious tracking error and initial fluctuation can be observed, and the RMS value of e_k during the iteration process is higher than that of adopting initialization learning. This proves the effectiveness of the proposed ILC strategy.

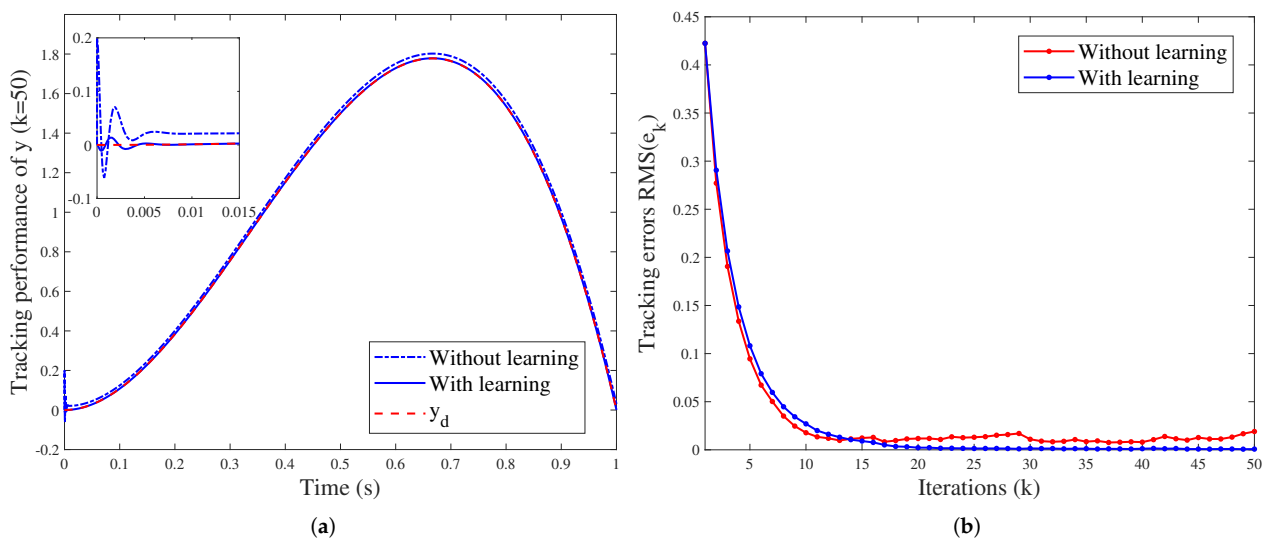


Figure 7. System performance with/without the initialization learning strategy ($k = 50$): (a) The tracking performance after 50 iterations. (b) Convergence of the RMS value of the tracking error $\text{RMS}_{t \in [0,1]}(e_k(t))$.

6. Conclusions

This paper discusses the impact of system initialization on ILC performance for initialized fractional order systems, and investigates strategies to improve system convergence. First, under the condition of iteration-varying initialization, initial shift and channel disturbances, a novel robust ILC convergence condition is strictly derived by applying the close-loop D^α -type updating law. Second, the bounds of the tracking errors are theoretically proven to be positively correlated with the degree of initialization non-repetition. Third, a novel initialization learning algorithm is proposed to improve the initialization condition, and thereby maintain the perfect ILC tracking performance. The proposed ILC scheme includes different initialization scenarios and has good physical interpretability, and its superiority and application potential are demonstrated through the two numerical examples.

Considering the theoretical basis and physical background of system initialization, there are still some potential open issues. As mentioned in Section 5, the design, identification and optimization of initialization path is still challenging. In the field of ILC, how to combine the reset operation with system initialization is also an interesting topic.

Author Contributions: Conceptualization, X.X. and J.L.; methodology, X.X.; validation, J.L. and J.C.; investigation, X.X.; resources, J.L. and J.C.; writing—original draft preparation, X.X.; writing—review and editing, J.L. and J.C.; visualization, X.X.; supervision, J.C.; project administration, J.L.; funding acquisition, J.L. and J.C. All authors have read and agreed to the published version of the manuscript.

Funding: This work was supported in part by the National Key Research and Development Plan of China under Grant 2022YFC2403103, and in part by the National Natural Science Foundation of China under Grant 62293504, 62293500.

Data Availability Statement: No new data were created or analyzed in this study.

Conflicts of Interest: The authors declare that they have no known competing financial interests or personal relationships that could have appeared to influence the work reported in this paper.

References

- Li, Y.; Chen, Y.; Ahn, H.S.; Tian, G. A survey on fractional-order iterative learning control. *J. Optim. Theory Appl.* **2013**, *156*, 127–140. [[CrossRef](#)]
- Zeng, J.; Wang, S.; Cao, W.; Zhang, M.; Fernandez, C.; Guerrero, J.M. Improved fractional-order hysteresis-equivalent circuit modeling for the online adaptive high-precision state of charge prediction of urban-electric-bus lithium-ion batteries. *Int. J. Circuit Theory Appl.* **2024**, *52*, 420–438. [[CrossRef](#)]
- Bhangale, N.; Kachhia, K.B.; Gómez-Aguilar, J. Fractional viscoelastic models with Caputo generalized fractional derivative. *Math. Meth. Appl. Sci.* **2023**, *46*, 7835–7846. [[CrossRef](#)]
- Chen, Y.Q.; Moore, K.L. On D^α -type iterative learning control. In Proceedings of the 40th IEEE Conference on Decision and Control, Orlando, FL, USA, 4–7 December 2001; pp. 4451–4456.
- Ye, Y.; Tayebi, A.; Liu, X. All-pass filtering in iterative learning control. *Automatica* **2009**, *45*, 257–264. [[CrossRef](#)]
- Xu, J.X.; Yan, R. On initial conditions in iterative learning control. *IEEE Trans. Autom. Control* **2005**, *50*, 1349–1354.
- Meng, D.; Moore, K.L. Robust iterative learning control for nonrepetitive uncertain systems. *IEEE Trans. Autom. Control* **2017**, *62*, 907–913. [[CrossRef](#)]
- Wei, Y.S.; Chen, Y.Y.; Shang, W. Feedback higher-order iterative learning control for nonlinear systems with non-uniform iteration lengths and random initial state shifts. *J. Frankl. Inst.* **2023**, *360*, 10745–10765. [[CrossRef](#)]
- Zhang, F.; Meng, D.; Li, X. Robust adaptive learning for attitude control of rigid bodies with initial alignment errors. *Automatica* **2022**, *137*, 110024. [[CrossRef](#)]
- Shokri-Ghaleh, H.; Ganjefar, S.; Shahri, A.M. Robust convergence conditions of iterative learning control for time-delay systems under random non-repetitive uncertainties. *IET Contr. Theory Appl.* **2023**, *17*, 144–159. [[CrossRef](#)]
- Ayatania, M.; Forouzanfar, M.; Ramezani, A. An LMI approach to robust iterative learning control with initial state learning. *Int. J. Syst. Sci.* **2022**, *53*, 2664–2678. [[CrossRef](#)]
- Chen, D.; Xu, Y.; Lu, T.; Li, G. Multi-phase iterative learning control for high-order systems with arbitrary initial shifts. *Math. Comput. Simul.* **2024**, *216*, 231–245. [[CrossRef](#)]
- Zhang, J.; Meng, D. Iterative Rectifying Methods for Nonrepetitive Continuous-Time Learning Control Systems. *IEEE T. Cybern.* **2023**, *53*, 338–351. [[CrossRef](#)] [[PubMed](#)]
- Yan, L.; Wei, J. Fractional order nonlinear systems with delay in iterative learning control. *Appl. Math. Comput.* **2015**, *257*, 546–552. [[CrossRef](#)]

15. Wang, L. Iterative Learning Consensus of Fractional-Order Multi-Agent Systems Subject to Iteration-Varying Initial State Shifts. *IEEE Access* **2019**, *7*, 173063–173075. [[CrossRef](#)]
16. Luo, D.; Wang, J.; Shen, D. Consensus tracking problem for linear fractional multi-agent systems with initial state error. *Nonlinear Anal.-Model Control* **2020**, *25*, 766–785. [[CrossRef](#)]
17. Zhao, Y.; Li, Y.; Zhang, F.; Liu, H. Iterative learning control of fractional-order linear systems with nonuniform pass lengths. *Trans. Inst. Meas. Control* **2022**, *44*, 3071–3080. [[CrossRef](#)]
18. Liu, S.; Wang, J. Analysis of iterative learning control with high-order internal models for fractional differential equations. *J. Vib. Control* **2018**, *24*, 1145–1161. [[CrossRef](#)]
19. Lan, Y.H.; Wu, B.; Luo, Y.P. Finite Difference Based Iterative Learning Control with Initial State Learning for Fractional Order Linear Systems. *Int. J. Control Autom. Syst.* **2022**, *20*, 452–460. [[CrossRef](#)]
20. Li, L. Rectified fractional order iterative learning control for linear system with initial state shift. *Adv. Differ. Equ.* **2018**, *2018*, 12. [[CrossRef](#)]
21. Zhao, Y.; Wei, Y.; Chen, Y.; Wang, Y. A new look at the fractional initial value problem: The aberration phenomenon. *J. Comput. Nonlinear Dyn.* **2018**, *13*, 121004. [[CrossRef](#)]
22. Maamri, N.; Trigeassou, J. Modelling and initialization of fractional order nonlinear systems: The infinite state approach. In Proceedings of the 10th International Conference on Systems and Control, Marseille, France, 23–25 November 2022; pp. 42–47.
23. Maamri, N.; Trigeassou, J.C. A Plea for the Integration of Fractional Differential Systems: The Initial Value Problem. *Fractal Fract.* **2022**, *6*, 550. [[CrossRef](#)]
24. Hinze, M.; Schmidt, A.; Leine, R.I. Numerical solution of fractional-order ordinary differential equations using the reformulated infinite state representation. *Fract. Calc. Appl. Anal.* **2019**, *22*, 1321–1350. [[CrossRef](#)]
25. Remache, D.; Caliez, M.; Gratton, M.; Santos, S.D. The effects of cyclic tensile and stress-relaxation tests on porcine skin. *J. Mech. Behav. Biomed. Mater.* **2018**, *77*, 242–249. [[CrossRef](#)] [[PubMed](#)]
26. López-Villanueva, J.A.; Rodríguez-Iturriaga, P.; Parrilla, L.; Rodríguez-Bolívar, S. A compact model of the ZARC for circuit simulators in the frequency and time domains. *AEU-Int. J. Electron. Commun.* **2022**, *153*, 154293. [[CrossRef](#)]
27. Li, Y.; Chen, Y.Q.; Ahn, H.S. Fractional order iterative learning control for fractional order system with unknown initialization. In Proceedings of the 2014 American Control Conference, Portland, OR, USA, 4–6 June 2014; pp. 5712–5717.
28. Xu, X.; Chen, J.; Lu, J. Fractional-order iterative learning control for fractional-order systems with initialization non-repeatability. *ISA Trans.* **2023**, *143*, 271–285. [[CrossRef](#)] [[PubMed](#)]
29. López-Villanueva, J.A.; Rodríguez Bolívar, S. Constant phase element in the time domain: The problem of initialization. *Energies* **2022**, *15*, 792. [[CrossRef](#)]
30. Kochubei, A.; Luchko, Y.; Machado, J.A.T. *Handbook of Fractional Calculus with Applications-Volume 1: Basic Theory*; De Gruyter: Berlin, Germany, 2019.
31. Lorenzo, C.F.; Hartley, T.T. Initialization of fractional differential equations: Background and theory. In Proceedings of the 2007 Proceedings of the ASME International Design Engineering Technical Conferences and Computers and Information in Engineering Conference, Las Vegas, NV, USA, 4–7 September 2007; pp. 1325–1333.
32. Lan, Y.H. Iterative learning control with initial state learning for fractional order nonlinear systems. *Comput. Math. Appl.* **2012**, *64*, 3210–3216. [[CrossRef](#)]
33. Ye, H.; Gao, J.; Ding, Y. A generalized Gronwall inequality and its application to a fractional differential equation. *J. Math. Anal. Appl.* **2007**, *328*, 1075–1081. [[CrossRef](#)]
34. Hosseini, S.M.; Wilson, W.; Ito, K.; Van Donkelaar, C.C. How preconditioning affects the measurement of poro-viscoelastic mechanical properties in biological tissues. *Biomech. Model. Mechanobiol.* **2014**, *13*, 503–513. [[CrossRef](#)]
35. Li, Y.; Chen, Y.Q.; Ahn, H.S. Fractional-order iterative learning control for fractional-order linear systems. *Asian J. Control* **2011**, *13*, 54–63. [[CrossRef](#)]
36. Hosseinasab, S.; Lin, C.; Pischinger, S.; Stapelbroek, M.; Vagnoni, G. State-of-health estimation of lithium-ion batteries for electrified vehicles using a reduced-order electrochemical model. *J. Energy Storage* **2022**, *52*. [[CrossRef](#)]
37. Beltempo, A.; Bonelli, A.; Bursi, O.S.; Zingales, M. A numerical integration approach for fractional-order viscoelastic analysis of hereditary-aging structures. *Int. J. Numer. Methods Eng.* **2020**, *121*, 1120–1146. [[CrossRef](#)]
38. Chen, Y.; Wen, C.; Gong, Z.; Sun, M. An iterative learning controller with initial state learning. *IEEE Trans. Autom. Control* **1999**, *44*, 371–376. [[CrossRef](#)]
39. Jesus, I.S.; Tenreiro MacHado, J. Development of fractional order capacitors based on electrolyte processes. *Nonlinear Dyn.* **2009**, *56*, 45–55. [[CrossRef](#)]
40. Gateman, S.M.; Gharbi, O.; Gomes de Melo, H.; Ngo, K.; Turmine, M.; Vivier, V. On the use of a constant phase element (CPE) in electrochemistry. *Curr. Opin. Electrochem.* **2022**, *36*, 101133. [[CrossRef](#)]
41. Kiniman, V.; Kanokwhale, C.; Boonto, P. Modeling cyclic voltammetry responses of porous electrodes: An approach incorporating faradaic and non-faradaic contributions through porous model and constant phase element. *J. Energy Storage* **2024**, *83*, 110804. [[CrossRef](#)]
42. He, X.; Sun, B.; Zhang, W.; Fan, X.; Su, X.; Ruan, H. Multi-time scale variable-order equivalent circuit model for virtual battery considering initial polarization condition of lithium-ion battery. *Energy* **2022**, *244*, 123084. [[CrossRef](#)]
43. Xue, D. *Fractional Calculus and Fractional-Order Control*; Science Press: Beijing, China, 2018.

44. Li, Y.; Zhao, Y. Memory identification of fractional order systems: Background and theory. In Proceedings of the 27th Chinese Control and Decision Conference, Qingdao, China, 23–25 May 2015; pp. 1038–1043.
45. Zhao, Y.; Li, Y.; Zhou, F. Adaptive memory identification of fractional order systems. *Discontin. Nonlinearity Complex.* **2015**, *4*, 413–428. [[CrossRef](#)]
46. Zhao, Y.; Wei, Y.; Shuai, J.; Wang, Y. Fitting of the initialization function of fractional order systems. *Nonlinear Dyn.* **2018**, *93*, 1589–1598. [[CrossRef](#)]

Disclaimer/Publisher’s Note: The statements, opinions and data contained in all publications are solely those of the individual author(s) and contributor(s) and not of MDPI and/or the editor(s). MDPI and/or the editor(s) disclaim responsibility for any injury to people or property resulting from any ideas, methods, instructions or products referred to in the content.